

1 **Global-scale Evaluation of SMAP, SMOS and ASCAT Soil Moisture Products using Triple** 2 **Collocation**

3 Fan Chen^{1,2}, Wade T. Crow¹, Rajat Bindlish³, Andreas Colliander⁴, Mariko S. Burgin⁴, Jun Asanuma⁵,
4 and Kentaro Aida⁵

5 ¹Science Systems and Applications, Inc., Greenbelt, MD, USA

6 ²USDA ARS Hydrology and Remote Sensing Laboratory, Beltsville, MD 20705, USA

7 ³NASA Goddard Space Flight Center, Greenbelt, MD 20771, USA

8 ⁴NASA Jet Propulsion Laboratory, California Institute of Technology, Pasadena, CA 91109, USA

9 ⁵University of Tsukuba, Tsukuba, Japan

10 **Abstract**

11 **Global-scale surface soil moisture products are currently available from multiple remote sensing platforms.**
12 **Footprint-scale assessments of these products are generally restricted to limited number of densely-**
13 **instrumented validation sites. However, by taking active and passive soil moisture products together with a**
14 **third independent soil moisture estimates via land surface modeling, triple collocation (TC) can be applied to**
15 **estimate the correlation metric of satellite soil moisture products (versus an unknown ground truth) over a**
16 **quasi-global domain. Here, an assessment of Soil Moisture Active Passive (SMAP), Soil Moisture Ocean**
17 **Salinity (SMOS) and Advanced SCATterometer (ASCAT) surface soil moisture retrievals via TC is presented.**
18 **Considering the potential violation of TC error assumptions, the impact of active-passive and satellite-model**
19 **error cross correlations on the TC-derived inter-comparison results is examined at *in situ* sites using quadruple**
20 **collocation analysis. In addition, confidence intervals for the TC-estimated correlation metric are constructed**
21 **from moving-block bootstrap sampling designed to preserve the temporal persistence of the original (unevenly-**
22 **sampled) soil moisture time-series. This study is the first to apply TC to obtain a robust global-scale cross-**
23

24 assessment of SMAP, SMOS and ASCAT soil moisture retrieval accuracy in terms of anomaly temporal
25 correlation. Our results confirm the overall advantage of SMAP (with a global average anomaly correlation of
26 0.76) over SMOS (0.66) and ASCAT (0.63) that has been established in several recent regional, ground-based
27 studies. SMAP is also the best-performing product over the majority of applicable land pixels (52%), although
28 SMOS and ASCAT each shows advantage in distinct geographic regions.

29

30 1. Introduction

31 As a key state variable in hydrological and meteorological modeling systems, the global
32 observation of soil moisture has become a major priority. Currently, several remote sensing
33 platforms provide continuous global surface (approximately 0-5 cm) retrievals: the National
34 Aeronautics and Space Administration (NASA)¶ Soil Moisture Active Passive (SMAP, 2015-),
35 the European Space Agency (ESA)¶ Soil Moisture Ocean Salinity (SMOS, 2009-), the European
36 Organisation for the Exploitation of Meteorological Satellites (EUMETSAT)¶ Advanced
37 SCATterometers (ASCAT, 2007-), and the Japanese Aerospace Exploration Agency (JAXA)¶
38 Advanced Microwave Scanning Radiometer 2 (AMSR2, 2012-). The accuracy of the satellite
39 soil moisture retrievals is typically described via their root-mean-squared-error (RMSE; e.g.
40 Brocca *et al.* 2010; Jackson *et al.* 2010; Kerr *et al.* 2016) or de-biased/unbiased RMSE
41 (ubRMSE; e.g. Colliander *et al.* 2017) versus ground-based observations at a footprint-scale.
42 However, difficulty in obtaining viable estimates of ground truth soil moisture at the satellite
43 footprint scale has limited past validation activities to a small number of locations (e.g., 60\$¶
44 core validation sites) and/or discrete time periods (e.g., field campaigns). The broader evaluation
45 of satellite soil moisture products (across regional or continental scales) is typically based on
46 comparisons with sparse ground soil moisture networks or modeled datasets (e.g., Paulik *et al.*
47 2014; González-Zamora *et al.* 2015; Piles *et al.* 2014; Al-Yaari *et al.* 2014; Polcher *et al.* 2016;

48 Kim *et al.* 2018). Naturally, such comparisons are unable to provide direct validation metrics
49 relative to the ground truth, but rather metrics against a chosen reference dataset with unknown
50 errors at the footprint-scale of satellite retrievals. For example, correlation coefficient metrics
51 obtained from comparing with point-scale ground observations have been shown to
52 underestimate the correlation between retrievals and true soil moisture values (Chen *et al.* 2017).

53 Initially designed for obtaining the calibration constants against a reference dataset in satellite
54 wind speed products, the triple collocation (TC) (Stoffelen 1998) technique provides a solution
55 to such challenge. In particular, TC can be applied to the estimate error variances of a
56 geophysical measurement system and has become an important tool for satellite soil moisture
57 assessments (e.g., Zwieback *et al.* 2012; Dorigo *et al.* 2010; Miralles *et al.* 2010; Draper *et al.*
58 2013). However, standard TC applications are limited to only providing relative error metrics. It
59 requires a reference dataset to be chosen from the three collocated data products, and the
60 resulting error variances are subject to the multiplicative and additive biases of the reference
61 dataset (Chen *et al.* 2017). Recently developed TC-based solution \pm the Extended Triple
62 Collocation, or ETC (McColl 2014) \pm IRUWKH3H DUVRQ Ψ FRUUHODWLRQFRHIILFLHQWPHWULFRQ
63 other hand, does not require a reference dataset and yields an absolute estimate of the temporal
64 correlatioQEHWZHHQWKHSURGXFWXQG HUHDOXDWLRQDQG WKHXQNQRZQWUXWK3H DUVRQ
65 coefficient is a widely reported metric for satellite soil moisture and an appropriate metric for
66 summarizing retrieval value in a data assimilation context (Reichle *et al.*, 2008). In this analysis,
67 we adopt the ETC solution and conduct an assessment and inter-comparison of the SMAP Level
68 3, SMOS Level 3 and ASCAT Level 2 soil moisture products based on the correlation metric
69 (R). Until recently, relatively few studies have been conducted to evaluate satellite soil moisture
70 products at a continental scale (e.g. Draper *et al.* 2013; Leroux *et al.* 2013) using TC. To the best

71 of our knowledge, this study is the first attempt to apply TC to obtain the footprint-scale
72 correlation metric for SMAP observations at quasi-global scale, and compare it directly with soil
73 moisture retrievals from SMOS and ASCAT.

74

75 Our basic strategy for applying TC is to employ soil moisture data triplets comprising a passive
76 microwave product (SMAP or SMOS), an active remote sensing product (ASCAT), and a land
77 surface model product. TC is based on a fundamental assumption that each of these products
78 contain uncorrelated errors. However, recent works have identified non-negligible error
79 correlation in soil moisture products acquired from active and passive microwave sources
80 (Gruber *et al.* 2016b; Pierdicca *et al.* 2017). This suggests that it is necessary to examine the
81 impact of violating this assumption on SMAP-ASCAT and SMOS-ASCAT-based TC analyses.
82 Therefore, we also apply the least-squares quadruple collocation solution (QC, Pierdicca *et al.*
83 2015) to estimate the error cross-correlations at over 200 sparse ground observation sites to
84 further evaluate the robustness of our global TC analysis strategy.

85 This paper is organized as follows. Section 2 reviews the TC and quadruple collocation (QC)
86 methodologies and data-processing procedures as well as the use of moving-block bootstrap re-
87 sampling to obtain confidence intervals for TC-derived R . Section 3 describes the remote
88 sensing, land surface modeling and ground observation datasets used in the analysis. Section 4
89 presents the QC results at sparse network sites and discusses the sensitivity of the TC analysis to
90 both non-zero error cross-correlation between active and passive satellite soil moisture products
91 and our choice of a particular land surface model dataset. Results and discussions of global

92 comparison of SMAP, SMOS and ASCAT soil moisture via TC are presented in Sections 5 and
93 6, respectively.

94

95 **2. Methodologies**

96 **2.1 Extended Triple Collocation**

97 In soil moisture validation and comparison studies, TC has typically been applied to estimate the
98 random error variance of a particular soil moisture dataset. In contrast, the extended triple
99 collocation (ETC) approach (McColl 2014) solves for the correlation between a dataset and the
100 unknown truth. As in TC, it requires three collocated, independent measurement systems (X , Y ,
101 Z , in our case representing: a passive satellite retrieval, an active satellite retrieval and a model
102 product, respectively) that describe the same geophysical variable (in this case - average surface
103 soil moisture of the satellite grid cell, which is approximately $40 \times 40 \text{ km}^2$). ETC is based on the
104 following assumptions: 1) all three datasets are linearly related to the true state (T); 2) zero error
105 cross-correlation exists between X , Y and Z ; and 3) zero correlation exists between errors and T
106 and 4) the stationary of signal and error statistics (Gruber *et al.* 2016a; Draper *et al.* 2013;
107 Zwieback *et al.* 2012). If these assumptions hold, the correlation between X and the T can be
108 estimated as

$$109 \quad \frac{\text{Cov}(X, T)}{\text{Var}(X)} \quad (1)$$

110 where $\text{Cov}(X, T)$ is the covariance of X and T , and $\text{Var}(X)$ is the variance of X . Analytical details for
111 deriving (1) from the classic TC method (Stoffelen 1998) can be found in McColl (2014).

112 To ensure consistency with the assumption listed above, seasonal signals are commonly removed
113 from the raw time-series of each product prior to the application of TC (Gruber *et al.* 2016a; Dorigo
114 *et al.* 2010; Su and Ryu, 2015). Here, anomaly time series are generated by removing the average
115 value of a 30-day moving window centered upon the data point being treated (i.e. from day -14 to
116 day +15). Given the potential temporally sparse nature of satellite retrievals, a minimum of 3
117 observations is required in each of the first and second halves of the 30-day window, in addition
118 to the data point being treated itself. This particular anomaly definition, versus the alternative
119 definition of deviations from a long-term seasonal climatology, has less stringent requirements
120 regarding the length of datasets, which is usually the limiting factor in the application of TC in
121 satellite products. While the removal of low-frequency variability has been shown to improve the
122 robustness of TC results (Chen *et al.* 2017), it renders our particular ETC approach insensitive to
123 (potentially-important) error in low-frequency and/or seasonal soil moisture dynamics. The
124 implications of this will be discussed below.

125 ETC-based estimates of correlation are considered viable when: 1) the collocated triple time series
126 is comprised of at least 50 data points; 2) positive correlation is found between each of the three
127 input anomaly time-series, and 3) ETC correlation outputs are real and positive for each of the
128 three datasets. All other ETC correlation estimates are masked. The positive correlation
129 requirement between input datasets (#2 above) is necessary to avoid ambiguity since ETC is unable
130 to resolve the sign of the output R values (McColl 2014). This limitation results in the exclusion
131 of pixels in certain regions where active and passive soil moisture retrievals are negatively
132 correlated (see additional discussion in Section 5).

133 **2.2 Estimation of error cross-correlation: Quadruple collocation**

134 As noted above, a potential source of error for the TC analysis is the presence of error cross-
135 correlation (ECC) between the soil moisture datasets, especially between active and passive
136 remote sensing products. Non-zero ECC violates the underlying TC assumptions and can lead to
137 biased TC results. In past studies, ECC was typically assumed to be zero between all products
138 (e.g., Leroux *et al.* 2013). However, recent works have revealed the presence of non-zero ECC
139 between active and passive soil moisture retrievals (Gruber *et al.* 2016b; Pierdicca *et al.* 2017).
140 Therefore, it is prudent to re-examine ECC levels in SMAP-ASCAT and SMOS-ASCAT soil
141 moisture data pairs utilized here.

142 The TC algorithm can be extended to include a fourth dataset (i.e., quadruple collocation, or QC)
143 and the error variances can be estimated with a least squares solution (Pierdicca *et al.* 2015) with
144 the same TC assumptions. Furthermore, the zero ECC assumption can be relaxed, and \pm on the
145 condition that only one pair within of the four datasets have non-zero ECC \pm estimates of ECC
146 can be obtained from the least-squares solution (Zwieback *et al.* 2012; Gruber *et al.* 2016b).

147 Here we adopt the formulation in Gruber *et al.* (2016b) to estimate the error cross-correlation
148 between the active (ASCAT) and passive (SMAP, SMOS) soil moisture datasets and assess the
149 impact of such cross-correlation on TC results. The QC analysis is conducted at sparse soil
150 moisture network sites where ground observations can serve as the fourth soil moisture dataset.
151 The QC formulation also provides estimates of the error variances of each dataset. In certain
152 cases, such estimates will be more accurate than those obtained from TC since QC can account
153 for the presence of non-zero ECC within a particular pair of collocated datasets (Yilmaz and
154 Crow, 2014).

169 **2.3 Confidence interval from moving block bootstrapping**

170 Using collocated surface soil moisture retrievals from passive (SMAP or SMOS) and active
171 (ASCAT) sensors and a land surface modeling product, the correlation metric of the three
172 satellite products (versus an unknown truth) can be estimated via TC at a quasi-global scale.

173 However, considerable sampling errors are expected in TC results, especially when the length of
174 the analysis is shortened to accommodate new satellite products (e.g., the two years of SMAP
175 considered here). Therefore, it is critical to account for sampling uncertainties when making
176 comparisons between the satellite products.

177 Here, such uncertainties are quantified via bootstrap re-sampling at each pixel to construct the
178 confidence interval (CI) of TC estimates. As noted earlier, auto-correlation in time-series will
179 reduce the effective sample size and thus underestimate the probability that the original bootstrap
180 confidence interval contains the true statistical property (Zwiers, 1990; von Storch and Zwiers,
181 1999). Since soil moisture time series typically contain large amounts of temporal auto-
182 correlation, this effect should be considered when generating boot-strapped errors estimates for
183 soil moisture TC results. Although mean 30-day signals have been removed from the original
184 time-series, our analysis suggests the resulting anomaly time-series still contains significant first-
185 order autocorrelation (not shown). This impact also applies for correlation estimated by ETC

186  correlation coefficient

187 formula from two to three time series members (McColl, 2014). A solution is proposed in
188 Mudelsee (2002, 2010) where a pair-wise moving block bootstrap (MBB) re-sampling technique
189 is applied to obtain a robust estimate of the confidence intervals IRU3HDUVRQWFRUUHODWLRQ
190 coefficient in serially-correlated time-series.

191 Here, we have adapted the MBB method introduced in Ólafsdóttir and Mudelsee (2014) for the
 192 bi-variate correlation problem to the triple collocation problem to construct the confidence
 193 interval of the ETC correlation results. In each iteration of the re-sampling procedure, MBB is
 194 applied to draw blocks of data triplets from the original time series samples to form samples that
 195 preserve the temporal persistence of the original data. Block length is determined from the
 196 equivalent autocorrelation coefficient of the three anomaly time-series (i.e., ETC inputs) which is
 197 calculated from individual persistence time, τ_i , of the three time-series. Persistence times are then
 198 estimated by minimizing the sum of squares:

$$199 \quad \sum_{i=1}^n (x(i) - \bar{x})^2 = \min \quad (4)$$

200 where n is the length of the time-series, $x(i)$ is the i th data point (i.e. soil moisture anomaly) and
 201 $t(i)$ is the linear time point (in unit of day) with uneven spacing, which is typical of satellite
 202 retrievals. Note that although the land surface model time-series are evenly spaced with sub-daily
 203 frequency, only the data points that temporally matched to the satellite retrievals are considered
 204 and thereby treated as an unevenly-spaced time series. The equivalent AR(1) autocorrelation
 205 coefficient is given by $\hat{\rho} = \frac{\sum_{i=1}^{n-1} (x(i) - \bar{x})(x(i+1) - \bar{x})}{\sum_{i=1}^n (x(i) - \bar{x})^2}$, where \bar{x} is the average time
 206 spacing. The autocorrelation coefficient is then bias-corrected to approximate the AR(1) process
 207 with an even time-spacing:

$$208 \quad \hat{\rho}_{\text{bias-corrected}} = \frac{\hat{\rho}}{1 - \hat{\rho}} \quad (5)$$

209 A joint, bias-corrected equivalent autocorrelation coefficient for the triple collocation analysis is
 210 given by

$$211 \quad \hat{\rho}_{\text{joint}} = \frac{\hat{\rho}_1 + \hat{\rho}_2 + \hat{\rho}_3}{3} \quad (6)$$

212

213 The optimal block length is then estimated as

$$214 \quad \tau = \text{NINT} \left(\frac{1}{\sqrt{\lambda}} \right) \quad (7)$$

215 where NINT denotes rounding to the nearest integer. Overlapping blocks of data triplets with the

216 length of τ are then extracted from the match-up anomaly time-series and then randomly

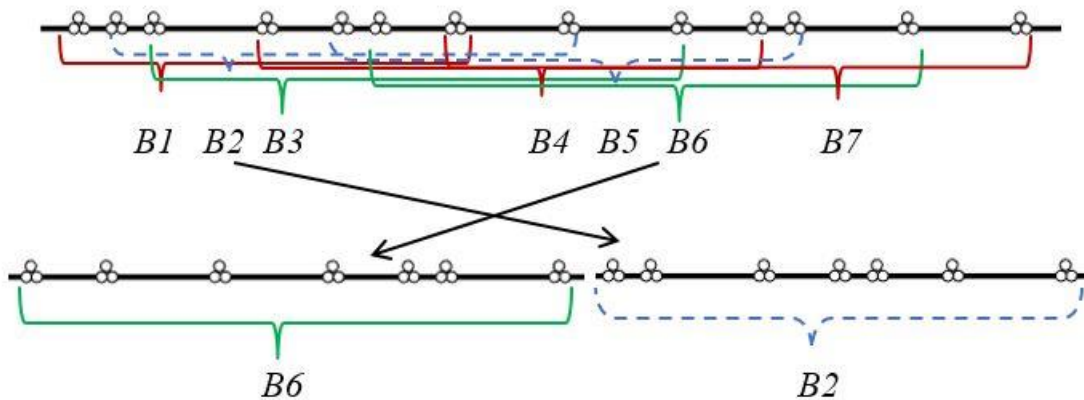
217 drawn with replacement to be concatenated until the original data length is reached (see Figure 1

218 for an illustration of this procedure). Extra data points in the end of the newly-formed bootstrap

219 sample are trimmed. The re-sampling procedure is repeated 1000 times in each grid pixel.

220 Estimated 95% confidence intervals for each correlation coefficient are defined as the range

221 between 2.5th and 97.5th percentile of the bootstrapped sampling distribution.



222

223 **Figure 1.** Schematic diagram of moving block bootstrapping for the case $\tau = 7$ applied to a temporally

224 sporadic time series of available soil moisture triplets. Overlapping data blocks from the original time

225 series (top) are drawn randomly with replacement and then concatenated to generate a new bootstrap

226 resample (bottom).

227

484 and ASCAT (averaged from SMAP- and SMOS-based TC) retrievals over common pixels are
485 0.76, 0.66 and 0.63, respectively.

486

487

488 **Figure 9.** Comparison of TC-estimated correlation coefficients between the satellite retrieval products.

489 Color shade indicates the product that obtains higher R in more than 95% of the bootstrap re-sampling

490 runs in a given grid cell. All areas of non-significant differences are masked. Plotted results are based on
491 the following triplets: a) [SMAP-ASCAT-ECMWF] (for SMAP) vs. [SMOS-ASCAT-ECMWF] (for
492 SMOS); b) [SMAP-ASCAT-ECMWF] (for SMAP and ASCAT); and c) [SMOS-ASCAT-ECMWF] (for
493 SMOS and ASCAT).

494

495 As noted in Section 4, it is likely that R values in Figures 8 and 9 are uniformly biased high (on
496 the order of 0.05 to 0.10 [-]) due to low amounts of ECC in SMAP-ASCAT and SMOS-ASCAT
497 pairs. However, relative R comparisons between products are expected to be more robust.
498 Qualitative comparisons between the satellite products are presented in Fig. 9, in which only
499 pixels with 95% significance of comparison are shown. Superiority at 95% significance is
500 achieved when one product has higher R value in more than 95% of the bootstrap re-samples.
501 Each bootstrap replicate is treated as an independent sample and the i th sample TC result for
502 SMAP is compared with the i th sample result for SMOS. In this way, approximately two-thirds
503 of the pixel-wise R differences are identified as being significant (see Table 2).

504 The two L-band passive soil moisture products are compared in Fig. 9a. SMOS out-performs
505 SMAP in areas of the Western United States, Southern Argentina, Central Asia and Eastern
506  dominate the rest of the globe. Globally, the SMAP
507 correlation is significantly higher than SMOS in 47% of the land pixels where comparisons are
508 available, while SMOS is significantly higher in 14% of the pixels (Table 2). In areas of
509 generally strong RFI pollution (e.g., Europe), the aggressive RFI mitigation efforts applied to
510 SMAP retrievals (Mohammed *et al.* 2016; Johnson *et al.* 2016; Piepmeier *et al.* 2017) may
511 explain their superior performance versus SMOS.

532 The SMOS ASCAT snowpack SMAP snowpack SMOS snowpack has been impacted by (somewhat
536 SMOS) relationships regarding data filtering most of the United States, Central Asia, and some
537 Australia, where ASCAT is better than SMOS data of Northern China, West and Far East (noting
538 SMOS suffers DOX threshold $(0.04 \text{ m}^3/\text{m}^3)$ at (Core) Argentina, and West SMOS DOX at (Core) (noting
539 both products) is applied extensively to a limited and relatively small area, as the analysis in Fig 9c TC. As
540 suggests that Table 2, more than 5000 pixels (or 14.4%) were firmly established physical DOX regions.
548 The spatial pattern of the TC SMOS-ASCAT-EGMWF analysis AR results show (Table 4) which
542 defines SMOS (DOX-ASCAT) with the Molar Light Retention in the SMAP for Research and
540 Application (MERRA-2) and DOX factor $0.04 \text{ m}^3/\text{m}^3$ to use (except in a worst SMAP similar 7% of Argentina
544 where SMOS is a better pixel), and better with MERRA-2 and the ASCAT SMOS better' pixels
542 as much (only ~2% pixels affected). In addition, only 0.3% of the common pixels change from a
545 Table 2. Pair-wise comparisons between TC-estimated correlation coefficients for various satellite
543 'SMOS better' to a 'SMAP better' category when the DOX threshold is relaxed from $0.04 \text{ m}^3/\text{m}^3$
546 products. The significance of differences is assessed using a 95% confidence threshold and the boot-
547 strapping approach described in Section 2.3. Percentages are out of all global land pixels with viable TC
548 SMOS performance relative to SMAP.

526	C-band active scatterometer retrievals from ASCAT SMOS performed by SMAP in most areas				
527	except for Northeastern China, Southern Argentina, and Southern Australia, where ASCAT				
528	retrievals demonstrate higher R (Fig. 9b). ASCAT R is significantly higher than SMAP R in only	47%	31%	14%	17%
529	14% of the pixels where TC results are available, while SMAP is significantly better than	40%	23%	17%	20%
530	ASCAT at more than 50% of the available global land pixels. Note that both SMOS and ASCAT				
531	SMAP vs. ASCAT data used here were subject to processing errors due to grid transformation (to the SMAP native	53%	19%	14%	14%
532	grid), which may cause slight under-performance and benefit SMAP in these comparisons.				
533	However, the slight global superiority of SMAP relative to SMOS is consistent with SMAP				
534	validation results at core validation sites (Chan <i>et al.</i> 2016).				
549		4P	$^3/\text{m}^3$ 4;P	$^3/\text{m}^3$	

550

551

552

553 **Figure 10.** The satellite product (SMAP, SMOS or ASCAT) with the highest single-run TC-based
554 correlation coefficient.

555

556 A map showing the best-performing satellite product is presented in Fig. 10. Note that regions
557 with dense vegetation are largely masked due to a lack of successful retrievals. Likewise, in arid
558 regions such as the Sahara Desert and Great Basin Desert, earlier studies have revealed poor or
559 even negative correlation between active and passive products (de Jeu *et al.* 2008; Pierdicca *et*
560 *al.* 2013; Burgin *et al.* 2017). This limits the area over which TC can be performed due to the
561 masking of pixels where negative mutual correlation exists among the input datasets (see Section
562 2.1). As indicated above, ASCAT R values obtained from SMAP- and SMOS-based TC analyses
563 are averaged for comparison. Overall, SMAP and SMOS are superior to ASCAT in most areas of
564 North America, Europe, Southern Asia and Eastern Australia. The significant overlap of

585 geographic regions where both passive satellite and active satellite data are available, each grid pixel with the highest the
 586 of correlation between SMAP and SMOS for a pixel is distributed by Burign of *et al.* (2017) on ASCAT is then
 589 generally higher than SMAP and SMOS for a pixel is distributed by Burign of *et al.* (2017) on ASCAT is then
 590 of South America (mainly Argentina) and Southwestern Australia. As in Fig. 9, SMOS has
 591 higher R than SMAP in the Western United States, Central Asia and most inland pixels of
 592 Eastern Australia. Overall, SMAP ranks highest in 52% of the pixels with viable TC results (see
 593 Section 2.1) whereas SMOS and ASCAT each does in 24% of these pixels.

592 positive error cross-correlation is found to exist between ASCAT and both SMAP and SMOS

595 which suggests that TC-estimated R for the three satellite-based products may be positively

596 6. Summary

596 biased. However, since this bias is small and approximately equal for all three products, the
 597 In this analysis, a global assessment and comparison of SMAP (L2 passive), SMOS (L3) and
 598 ASCAT (L2) surface soil moisture products is performed based on the correlation metric (R)
 599 limited impact associated with potential satellite-model error cross-correlations. Recent findings
 600 obtained via triple collocation (TC). In order to produce robust TC results, R is estimated
 601 by Pierdicca *et al.* (2017) using a novel extended QC algorithm and 15 months of satellite and
 602 following removal of low-frequency variability in the soil moisture time series and therefore
 603 model data reveals weak SMAP-SMOS ECC that is lower than the SMAP-ASCAT ECC found.
 604 reflects the R of soil moisture anomalies relative to a 30-day moving temporal average. Given
 605 Such findings suggest the further potential of using SMAP and SMOS together in TC in future
 606 that low-frequency error sources have been previously identified in certain remotely-sensed soil
 607 analyses. Finally, the sensitivity of SMOS TC results to the specification of the DQX threshold is
 608 moisture products (Wagner *et al.*, 2014), this focus on solely high-frequency noise represents a
 609 shown to be low.

581 limitation in our approach. Nevertheless, sensitivity experiments suggest that our global TC

604 To the best of our knowledge, this study is the first to present a global-scale triple collocation
 582 results are relatively insensitive to changing the size of the moving window from 30 to 60 days

605 analysis that compares the footprint-scale correlation metric of SMAP with SMOS and ASCAT
 583 (not shown).

606 soil moisture products. Results suggest that, out of these three products, SMAP has the highest

584 In addition, when comparing satellite products, it is critical to account for the sampling
 607 global average R (0.76, SMOS: 0.66, ASCAT: 0.63) and is the superior product for the majority

585 uncertainties due to sparse temporal availabilities or suboptimal retrieval conditions. To this end,
 608 (52%) of global land pixels with a viable TC result. This finding is consistent with several recent

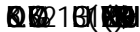
586 a moving-block bootstrap re-sampling approach, with emphasis on preserving the temporal
 609 validation studies (e.g. Kumar *et al.* 2017; Montzka *et al.* 2017; Pierdicca *et al.* 2017; Kim *et al.*

630 2018) for the SMAP, using it for validation purposes. Research SMAP data is only provided by the
633 National Aeronautics and Space Administration (NASA) Soil Moisture Active Passive (Kumar
632 et al. 2017) & Liu, B., Zsif, V. a P. H. F. H. J. W. K. P. S. R. Q. W. K. H. G. D. S. B. G. F. H. D. Q. F. H. P. T. H. D. P. \$ G
635 Soil Moisture Active Passive (SMAP) data is provided by the California Institute of Technology (Caltech) and the NASA Probes
636 (CRNP, including some of the COSMOS stations used here) across five continents, SMAP
637 outperformed other satellite products including AMSR2, SMOS and ASCAT (Montzka et al
638 **References** nevertheless, each of the three satellite retrieval products (SMAP, SMOS and ASCAT)
617 were found to be superior (to the other two) in specific global land regions. Therefore, the global
639 Al-Yaari, A., Wigneron, J.-P., Ducharne, A., Kerr, Y. H., Wagner, W., De Lannoy, G., Reichle, R., Al
618 inter-comparison maps in Figures 9 and 10 provide useful information for regional-scale
640 Bitar, A., Dorigo, W., Richaume, P., and Mialon, A. (2014). Global-scale comparison of passive (SMOS)
619 applications such as the choice of dataset for assimilation into rainfall-runoff models
642 and active (ASCAT) satellite based microwave soil moisture retrievals with soil moisture simulations
620 (MERRA-Land), *Remote Sens. Environ.* 52, 614-626.
621 In closing, it should be noted that all products considered here are subject to frequent re-
622 processing and algorithm improvements: For example, a new global daily SMOS SM product --
644 Scipal, K. (2009). A revised hydrology for the ECMWF model: Verification from field site to terrestrial
622 the SMOS-INRA-CESBIO (SMOS-IC) product was recently released and shown to yield
645 water storage and impact in the ECMWF-IFS, *J. Hydrometeorol* 10, 623-643.
623 generally higher correlations versus ground observation versus the v300 SMOS Level 3 soil
646 Bell, J. E., Palecki, M. A., Baker, C. B., Collins, W. G., Lawrimore, J. H., Leeper, R. D., Hall, M. B.,
624 moisture product considered here (Fernandez-Moran et al., 2017). Comparable enhanced SMAP
647 Kochendorfer, J., Meyers, T. P., Wilson, T. and Diamond, H. J. (2013). U.S. Climate Reference Network
625 soil moisture products are likely to arise in the foreseeable future. Therefore, the cross evaluation
648 soil moisture and temperature observations, *J. Hydrometeorol* 14(3), 977-988.
626 efforts described here are, in reality, an on-going effort requiring updating as improved products
649 Brocca, L., Melone, F., Moramarco, T., Wagner, W., and Hasenauer, S. (2010). ASCAT soil wetness
627 are released.
650 index validation through in situ and modeled soil moisture data in central Italy, *Remote Sens. Environ.*
628 **Acknowledgements**
651 114(11), 2745-2755.
629 ECMWF soil moisture field was provided by European Centre for Medium-range Weather and grids
630 Forecasting (ECMWF) Discrete Global Grids, National Center for Space Global Modeling and Analysis.
631 Forcast, N. M. (Ed.) Discrete Global Grids, National Center for Space Global Modeling and Analysis.
634 Santa Barbara, CA, USA
635 Assimilation Office. Ground soil moisture measurements were contributed by individual

655 Burgin, M., Colliander, A., Njoku, E. G., Chan, S. K., Francois, C., Kerr, Y. H., Bindlish, R., Jackson, T.
656 J., Entekhabi, D., Yueh, S. H. (2017). A comparative study of the SMAP passive soil moisture product
657 with existing satellite-based soil moisture products, *IEEE Trans. Geosci. Remote Sens.*, 55(5), 2959-2971.

658 Calvet, J.-C., Fritz, N., Froissard, F., Suquia, D., Petitpa, A., and Pigué, B. (2007) In situ soil moisture
659 observations for the CAL/VAL of SMOS: the SMOSMANIA network, *2007 IEEE Int. Geosci. Remote*
660 *Sens. Symposium*, Barcelona, Spain, 1196-1199.

661 Chan S., and Dunbar, R. S. (2015). SMAP Level 2 passive soil moisture product specification document,
662 JPL D-72547, Jet Propulsion Laboratory, Pasadena, CA, USA. Available:
663 [https://nsidc.org/sites/nsidc.org/files/technical-references/SMAP%20L2_SM_P%20Beta-](https://nsidc.org/sites/nsidc.org/files/technical-references/SMAP%20L2_SM_P%20Beta-Level%20PSD%20%28PRIMARY%29.pdf)
664 [Level%20PSD%20%28PRIMARY%29.pdf](https://nsidc.org/sites/nsidc.org/files/technical-references/SMAP%20L2_SM_P%20Beta-Level%20PSD%20%28PRIMARY%29.pdf)

665  (2016). Assessment of the SMAP Passive Soil Moisture Product, *IEEE Trans. Geosci. Remote Sens.*, 54.
666 1-14.

668 Chen, F., Crow, W. T., Colliander, A., Cosh, M., Jackson, T. J., Bindlish, R., and Reichle, R. (2017).
669 Application of triple collocation in ground-based validation of soil moisture active/passive (SMAP) data
670 products. *IEEE J. Sel. Topics Appl. Earth Obs. Rem. Sens.*, 10 (2), 489-502.

671 Chew, C. C., Small, E. E., Larson, K. M., and Zavorotny, V. U. (2014). Effects of near-surface soil
672 moisture on GPS SNR data: development of a retrieval algorithm for soil moisture, *IEEE Trans Geosci*
673 *Remote Sens*, 52, 537±543.

674 Colliander, A-DFNVRQ7-%LQGOLVK5&KDQ6'DV1.LP6%«XHK69DOLGDWLRQ
675 of SMAP surface soil moisture products with core validation sites, *Remote Sens. Environ.*, 191, 215-231.

676 de Jeu, R.A.M., Wagner, W., Holmes, T.R.H., Dolman, A.J., van de Giesen, N.C., and Friesen, J. (2008)
677 Global soil moisture patterns observed by space borne microwave radiometers and scatterometers,
678 *Surveys in Geophysics*, 29, 399-420. doi:10.1007/s10712-008-9044-0.

709 Drosch, M., Rosnay, P., Balsamo, G., Albritton, C. R., Muñoz-Sabido, C., Clayford, S., Kshirsagar, H., and Haidt, A. (2008) and
700 Mesoscale variables from Nonlinear Weather Prediction State Vector. *Geophys. Res. Lett.*, 35, L12205, doi:10.1029/2007GL032057. 167-
705 182.
687 Dorigo, W. A., Scipal, K., Parinussa, R. M., Liu, Y. Y., Wagner, W., de Jeu, R. A. M., and Naeimi, V.
702 (2009) From Global Mission to Global Data. In *Soil Moisture and Water Deficit: A Global Perspective*, Ed. C. S. M. O. S. A.,
703 M. S. G. O. J. (2010). Validation of Advanced Microwave Scanning Radiometer soil moisture products,
708 *IEEE Trans. Geosci. Remote Sens.*, 48(12), 4256-4272.
684 Draper, C., Reichle, R., de Jeu, R., Naeimi, V., Parinussa, R., and Wagner W. (2013). Estimating root mean
709 square error of remotely sensed soil moisture over continental scales. *Remote Sens. Environ.*, 137, 180-190.
710 2016-2018 and Validation for the L2/3_SM_P Version 4 and L2/3_SM_P_E Version 1 Data Products,
711 SMAP Project, IPL D-56297, Jet Propulsion Laboratory, Pasadena, CA, USA, available:
687 https://nsidc.org/sites/nsidc.org/files/files/D56297%20SMAP%20L2_SM_P_E%20Assessment%20Report%20Karrnan%20Inter%20based%20soil%20moisture%20analysis%20system%20for%20the%20operational%20ECMWF%20integrated%20forecast%20system.pdf
712 (1).pdf
688 System, *Geophys. Res. Lett.*, 36, L10401 doi:10.1029/2009GL037716.
713
714 Johnson, J. T., Mohammed, P. N., Piepmeyer, J. R., Bringer, A., and Aksoy, M. (2016). Soil Moisture : 7 (GHO
690 Entekhabi, D.; Njoku, E. 2. 1. HLOO 3 (. HOORJJ . + & URZ :
715 Active Passive (SMAP) microwave radiometer radio-frequency interference (RFI) mitigation: Algorithm
691 (2010). The Soil Moisture Active Passive (SMAP) mission, *Proc. IEEE*, 98(5), 704-716.
716 updates and performance assessment, *2016 IEEE Int. Geosci. Remote Sens. Symposium*, Beijing, China,
692 Fernandez-Moran, R., Al-Yaari, A., Mialon, A., Mahmoodi, A., Al Bitar, A., De Lannoy, G., Rodriguez-
717 123-124.
693 Fernandez, N., Lopez-Baeza, E., Kerr, Y., and Wigneron, J.-P. (2017). SMOS-IC: an alternative SMOS
718 Kaihotsu, I., Koike, T., Yamanaka, T., Fujii, H., Ohta, T., Tamagawa, K., Oyunbaatar, D., and Akiyama,
694 soil moisture and vegetation optical depth product. *Remote Sens.*, 9 (5), 457; doi:10.3390/rs9050457.
719 R. (2009). Validation of Soil Moisture Estimation by AMSR-E in the Mongolian Plateau, *J. Remote Sens.*
695 González-Zamora, A., Sánchez, N., Gumuzzio, A., Piles, M., Olmedo, E., and Martínez-Fernández, J.
720 *Soc. Japan*, 29, 271-281.
696 (2015). Validation of SMOS L2 and L3 soil moisture products over the Duero basin at different spatial
721 Kerr, Y. H., Al-Yaari, A., Rodriguez-Fernandez, N., Parrens, M., Molero, B., Leroux, D., Bircher, S.,
697 scales, *Int. Arch. Photogramm. Remote Sens. Spatial Inf. Sci.*, XL-7/W3, 1183-1188.
722 Mahmoodi, A., Mialon, A., Richaume, P., Delwart, S., Al Bitar, A., Pellarin, T., Bindlish, R., Jackson, T.
698 Gruber, A., Su, C.-H., Zwieback, S., Crow, W. T., Dorigo, W., and Wagner, W. (2016a). Recent advances
723 J., Rüdiger, C., Waldteufel, P., Mecklenburg, S., and Wigneron J.-P. (2016). Overview of SMOS
699 in (soil moisture) triple collocation analysis, *Int. J. Appl. Earth Obs. Geoinf.*, 45, part B, 200-211.
724 performance in terms of global soil moisture monitoring after six years in operation, *Remote Sens.*
700 Gruber, A., Su, C.-H., Crow, W. T., Zwieback, S., Dorigo, W. A., and Wagner, W. (2016b), Estimating
701 error cross-correlation in soil moisture data sets using extended collocation analysis, *J. Geophys. Res.*
702 *Atmos.*, 121, 1208-1219.

726 Kerr, Y. H., Jacquette, E., Al Bitar, A., Cabot, F., Mialon, A., Richaume, P., and Berthon, L. (2013). In
727 CBSA (Ed.), CATDS SMOS L3 Soil Moisture Retrieval Processor Algorithm Theoretical Baseline
728 Document (ATBD) CBSA, Technical Note (pp. 73). Toulouse: CESBIO.

729 Kerr, Y. H., Waldteufel, P., Wigneron, J. P., Martinuzzi, J. M., Font, J., and Berger, M. (2001). Soil
730 moisture retrieval from space: the soil moisture and ocean salinity (SMOS) mission, *IEEE Trans. Geosci.*
731 *Remote Sens.*, 39, 1729–1735.

732 Kim, H., Parinussa, R., Konings, A.G., Wagner, W., Cosh, M.H., Lakshmi, V., Zohaib, M., and Choi, M.
733 (2018). Global-scale assessment and combination of SMAP with ASCAT (active) and AMSR2 (passive)
734 soil moisture products, *Remote Sens. Environ.*, 204, 260-275, doi:10.1016/j.rse.2017.10.026.

735 . : K O L 0 6 F K U : Q 0 = U H G D 0 6 F K P L G W 18). Footprint W U L F K 3 D Q G
736 characteristics revised for field-scale soil moisture monitoring with cosmic-ray neutrons, *Water Resour.*
737 *Res.*, 51, 5772–5790.

738 Kumar, S. V., Dirmeyer, P. A., Peters-Lidard, C. D., Bindlish, R., and Bolten, J. (2017). Information
739 theoretic evaluation of satellite soil moisture retrievals, *Remote Sens. Environ.*, in press,
740 doi:10.1016/j.rse.2017.10.016.

741 Larson, K. M., and Nievinski, F. G. (2013). GPS snow sensing: results from the Earthscope Plate
742 Boundary Observatory, *GPS Solut.*, 17, 41–52.

743 Larson, K. M., Small, E. E., Gutmann, E., Bilich, A., Braun, J., and Zavorotny, V. (2008). Use of GPS
744 receivers as a soil moisture network for water cycle studies, *Geophys. Res. Lett.*, 35, L24405,
745 doi:10.1029/2008GL036013.

746 Leroux, D. J., Kerr, Y., Richaume, P., and Fieuzal, R. (2013). Spatial distribution and possible sources of
747 SMOS errors at the global scale, *Remote Sens. Environ.*, 133, 240-250.

769 Piepmeier, J. R., Focardi, 3 + R U J D Q . \$. Q X E O H - (K V D Q 1 / X F H \ - «
770 SMAP L-Band Microwave Radiometer: Instrument Design and First Year on Orbit, *IEEE Trans. Geosci.*
771 *Remote Sens.*, 55(4), 1954-1966.

772 Pierdicca, N., Pulvirenti, L., Fascetti, F., Crapolicchio R., and Talone, M. (2013). Analysis of two years
773 of ASCAT-and SMOS-derived soil moisture estimates over Europe and North Africa, *European J.*
774 *Remote Sens.*, 46:1, 759-773, doi:10.5721/EuJRS20134645.

775 Pierdicca, N., Fascetti, F., Pulvirenti, L., Crapolicchio, R., and Muñoz-Sabater, J. (2015). Quadruple
776 Collocation Analysis for Soil Moisture Product Assessment, *IEEE Geosci. Remote Sens. Lett.*, 12(8),
777 1595-1599.

778 Pierdicca, N., Fascetti, F., Pulvirenti, L., and Crapolicchio, R. (2017). Error characterization of soil
779 moisture satellite products: retrieving error cross-correlation through extended quadruple collocation,
780 *IEEE J. Sel. Topics Appl. Earth Obs. Rem. Sens.*, 10, 4552-4530, doi:10.1109/JSTARS.2017.2714025.

781 Piles, M., Sánchez, N., Vall-llossera, M., Camps, A., Martínez-Fernández, J., Martínez, J., and González-
782 Gambau, V. (2014). A Downscaling Approach for SMOS Land Observations: Evaluation of High-
783 Resolution Soil Moisture Maps Over the Iberian Peninsula, *IEEE J. Sel. Topics Appl. Earth Observ. Remote*
784 *Sens.*, 7(9), 3845-3857.

785 Polcher, J., Piles, M., Gelati, E., Barella-Ortiz, A., and Tello, M. (2016). Comparing surface-soil moisture
786 from the SMOS mission and the ORCHIDEE land-surface model over the Iberian Peninsula, *Remote*
787 *Sens. Environ.*, 174, 69-81.

788 Reichle, R.H., **Crow, W.T.**, Koster, R. D., Sharif, H. and Mahanama, S. (2008). Contribution of soil
789 moisture retrievals to land data assimilation products. *Geophys. Res. Lett.*, 35. L01404,
790 doi:10.1029/2007GL031986.

791

792 Reichle, R. H., De Lannoy, G. J. M., Liu, Q., Ardizzone, J. V., Chen, F., Colliander, A., Conaty, A.,
793 Crow, W., Jackson, T., Kimball, J., Koster, R. D., and Smith, E. B. (2016). Soil Moisture Active Passive
794 Mission L4_SM Data Product Assessment (Version 2 Validated Release). GMAO Office Note No. 12
795 (Version 1.0), 55 pp, NASA Goddard Space Flight Center, Greenbelt, MD, USA. Available:
796 http://gmao.gsfc.nasa.gov/pubs/office_notes.

797 Scott, B., Ochsner, T., Illston, B., Fiebrich, C., Basara, J. and Sutherland, A. (2013). New soil property
798 database improves Oklahoma Mesonet soil moisture estimates, *J. Atmos. Oceanic Technol.*, 30, 2585±
799 2595.

800 Shaefer, G. L., Cosh, M. H., and Jackson, T. J. (2007). The USDA Natural Resources Conservation Service
801 Soil Climate Analysis Network (SCAN), *J. Atmos. Oceanic Technol.*, 24, 2073-2077.

802 Stoffelen, A. (1998). Toward the true near-surface wind speed: error modeling and calibration using triple
803 collocation, *J. Geophys. Res.*, 103(C4), 7755-7766.

804 Su, C.-H. and Ryu, D. (2015). Multi-scale analysis of bias correction of soil moisture, *Hydrol.*
805 *Earth Syst. Sci.*, 19, no. 1,17-31.

806 von Storch, H., and Zwiers, F. W. (1999). Statistical analysis in climate research, Cambridge University
807 Press, Cambridge, UK, 484pp.

808 Wagner, W., Lemoine, G., and Rott, H. (1999). A method for estimating soil moisture from ERS
809 scatterometer and soil data, *Remote Sens. Environ.*, 70(2), 191-207.

810 Wagner, W., Brocca, L., Naeimi, V., Reichle, R., Draper, C., de Jeu, R., Ryu, D., Su, C. H., Western, A.,
811 Calvet, J. C., Kerr, Y. H., Leroux, D. J., Drusch, M., Jackson, T. J., Hahn, S., Dorigo, W., and Paulik, C.
812 ■ on Between SMOS, VUA, ASCAT, and ECMWF Soil Moisture
813 3023 *IEEE Trans. Geosci. Remote Sens.*, 52(3), 1901-1906.

814 Yilmaz, M. T., and Crow, W. T. (2014). Evaluation of assumptions in soil moisture triple collocation
815 analysis, *J. Hydrometeor.*, 15(3), 1293±1302.

862 SMOS); b) [SMAP-ASCAT-ECMWF] (for SMAP and ASCAT); and c) [SMOS-ASCAT-ECMWF] (for
863 SMOS and ASCAT).

864 **Figure 10.** The satellite product (SMAP, SMOS or ASCAT) with the highest TC-based correlation
865 coefficient (\bar{r} bootstrap mean).

